Investigation of mechanical and microstructural properties of friction stir welded dual phase (DP) steel

IOP Conf. Series: Materials Science and Engineering **629** (2019) 012010 doi:10.1088/1757-899X/629/1/012010

Investigation of mechanical and microstructural properties of friction stir welded dual phase (DP) steel

T Küçükömeroğlu[1,4], S M Aktarer[2] and G Çam[3]

[1]Department of Mechanical Engineering, Karadeniz Technical University, 61100 Trabzon, Turkey
[2]Department of Automotive Technology, Recep Tayyip Erdogan University, 53080 Rize, Turkey
[3]Department of Mech. Engineering, Iskenderun Technical University, 31200 İskenderun/Hatay, Turkey

E-mail: tkomer@ktu.edu.tr

Abstract. The application of dual phase (DP) steels has been increasing significantly in the automotive industry because of their high strength as well as good ductility, thus, cold formability. These steels are generally joined using conventional welding methods such as resistance spot welding and laser welding in the production of automotive parts. In recent years, several studies have been conducted to investigate the possibility of joining the advanced high-strength steels such as DP steels using the solid-state friction stir welding (FSW) method due to its advantages over conventional fusion joining methods such as metallurgical benefits, energy efficiency, and environmental friendliness. The aim of this study is to investigate the microstructure, hardness and tensile properties of friction stir welded DP 600 steel plates. Thus, 1.5 mm thick DP 600 steel plates were friction stir butt-welded by a tungsten carbide stirring tool consisting of a concave shoulder having a diameter of 14 mm and a conical pin (angle=30°) with a diameter and length of 5 mm and 1.25 mm, respectively. In the weld trials conducted, the tool was tilted 2° and the down-force of the tool was kept constant at 6 kN. The tool rotation and traverse speeds used in FSW trials were 1600 rpm and 170 mm.min-1, respectively. The microstructure of friction stir welded zone comprised of main martensite, bainite, and refined ferrite. The average hardness of the stir zone has increased to about 400 HV. The tensile specimens failed in the base plate away from the weld zone and tensile strength as high as that of the base plate was obtained from the welded specimens, i.e., about 640 MPa. However, the elongation of the welded plates was significantly reduced, i.e. about 55% of that of the base.

1. Introduction

Today, the automotive industry is increasingly focusing on reducing the dependence on fossil fuels, increasing security and increasing fuel economy. The use of advanced high strength steel (AHSS) in automotive parts has been a success in meeting the requirements of the lightweight and safe vehicle. Dual-phase (DP) steels which are one kind of the advanced high strength steels employed in the automotive industry consist of soft ferrite matrix contributing to ductility and a hard martensite phase distributed throughout the ferrite [1-3]. Dual-phase steels are the most commonly used in the automotive industry among advanced high-strength steels due to their high strength and good formability [4]. In many automotive applications such as door panels, roofs, and A and B columns, joining of dual phase steels is needed [5]. However, during the welding of the dual phase steels using conventional fusion

welding methods, undesirable hardness reduction occurs in the heat affected zone [6].

The friction stir welding (FSW), which is a new solid-state welding method originally developed for joining difficult-to-weld Al-alloys [7-12], are widely used to join several structural materials, such as pure Pb [13], Cu and Cu-alloys [14-16], Mg-alloys [10,17], similar and dissimilar Al-alloys [18-25] and even high melting temperature materials such as Ti-alloys and steels [9-11,26]. FSW results in lower residual stresses and distortion of the plates and the grain growth is kept to the lowest level in steels as in other structural materials due to the low heat input involved [10,11,25,27]. In recent years, many researchers have been working on joining of high strength steels via friction stir welding owing to its metallurgical advantages [28-30]. Most of the studies reported on advanced high strength steels have been conducted on friction stir spot welding [31-36]. The number of studies conducted on the friction stir butt welding of advanced high strength steels is very scarce [37-39]. Thus, there is still a need for a systematic study of the microstructure and mechanical properties of dual-phase steels joined with the friction stir welding. Therefore, the purpose of this study is to investigate the microstructure, microhardness and mechanical properties of DP 600 steel plates joined by FSW.

2. Experimental procedure

Hot rolled DP600 steel with a chemical composition of 0.060% C, 1.476% Mn, 0.330% Si, 0.045% Al, 0.040% Cu, 0.667% Cr, 0.034% Ni, 0.003% Mo, 0.062% P, 0.004% S and balance Fe was used in this study. DP600 steel sheet plates with dimensions of 200 mm × 50 mm × 1.5 mm were joined by FSW. The shoulder diameter, pin diameter and pin length of the tungsten carbide tool used for FSW are 14 mm, 5 mm, and 1.3 mm, respectively. The cone angle of the pin is 30 degrees. The tool rotation speed used was 1600 rpm and the traverse speed was 170 mm/min. The tool force was kept constant at 6 kN and tool tilt angle 2°. Optical microscopy (OM) and scanning electron microscope (SEM) was used for the investigation of the microstructures evolved in the FSW region. Tensile test specimens and metallographic examination samples were extracted from the joint by electro-discharge machine (EDM) method in a direction perpendicular to the welding direction as shown schematically in figure 1.

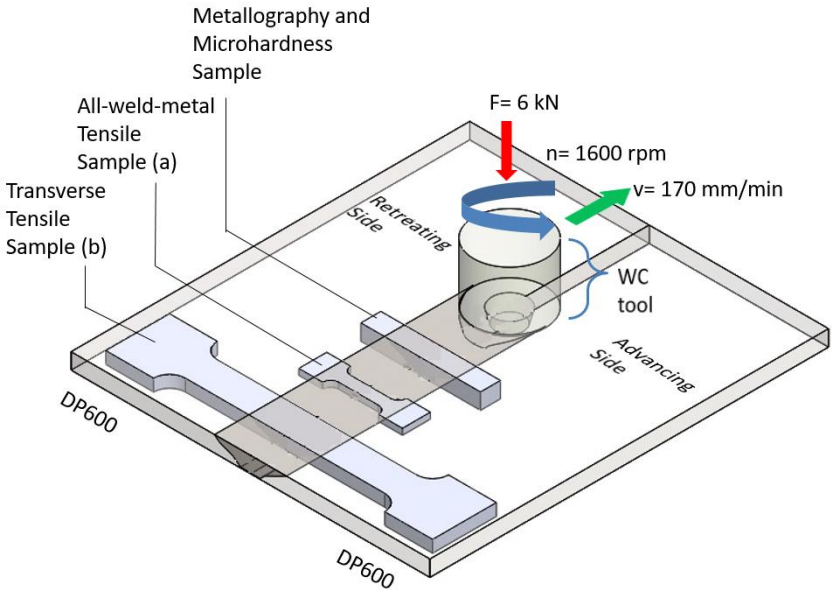

Figure 1. Schematic representation of the FSW trial and the extraction of the test samples (both transverse tensile and all-weld-metal tensile specimens) from the joint.

Transverse dog-bone-shaped tensile and all-weld-metal dog-bone-shaped tensile specimens with gage sections of 1.4 mm × 3 mm × 8 mm and 1.4 mm × 8 mm × 35 mm, respectively, were subjected to tensile testing. The tensile tests were carried out using an Instron-3382 universal test machine with a

video type extensometer at a strain rate of $5\times10^{-3}s^{-1}$. The metallography sample was etched for 20 s with 2% Nital (2 ml. HNO_3 + 98 ml. C_2H_6O) reagent after standard grinding and polishing. Vickers microhardness measurements were performed using 200 g load for 10s. In order to measure the temperatures that were experienced in various regions of the joint during the FSW, the thermocouples were located at the center of the stir zone and heat affected zone (figure 2(a)).

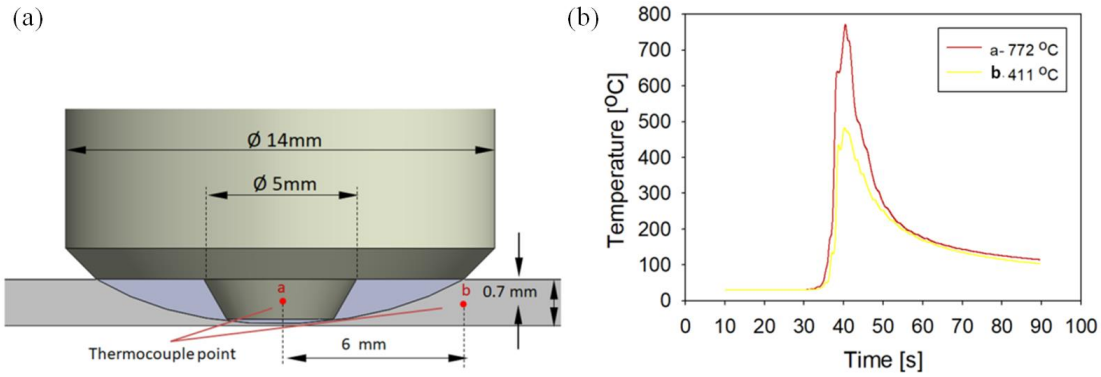

Figure 2. (a) The positions where the thermocouples were placed to measure the temperatures experienced in the FSW region (in both the SZ and HAZ regions) and (b) the corresponding temperature curves obtained from the SZ and HAZ regions.

3. Results and discussion

3.1. Microstructural aspects

The positions of the thermocouples placed in the stir zone (SZ) and the heat affected zone (HAZ) are shown in figure 2(a) and the temperature curves recorded from these regions during FSW are given in figure 2(b). As seen from these curves the peak temperature reached in the SZ during FSW was about 772°C.

As clearly seen from figure 3(a), no defects such as slot formation or microvoids were observed in the weld region. The microstructure of the DP 600 steel base plate consists of ferrite grains containing martensite islands (figure 3(b)). This microstructure has changed significantly after FSW. The microstructure of the stir zone was observed to be consisting of lath martensite (figure 3(c)) and bainite (figure 3(d)). The heat affected zone mainly consisted of tempered martensite (figure 3(e)). The average ferrite grain size of the DP 600 steel base plate was 6 µm and the martensite fraction was 25%. The microstructure evolved in the center of the stir zone after the FSW consisted of mainly lath martensite. Similarly, Ohashi *et al* [39] also reported that the microstructure formed in the SZ of DP 590 steel consisted of entirely lath martensite after the friction stir spot welding. The stir zone is exposed to both severe plastic deformation and friction heat due to the rotating tool during FSW. The peak temperature value of the stir zone center and HAZ were measured to be 772°C and 411°C, respectively. Therefore, it is said that the austenite can be transformed into martensite or bainite depending on the cooling rate during FSW. On the other hand, the formation of the bainite structure in the stir zone neighboring the HAZ region may be due to the decrease in the peak temperature experienced in this region and the plastic deformation taking place. Xie *et al* [40] also reported the formation of similar bainitic microstructure which they attributed to the low heat input because of insufficient plastic material flow and friction. Martensite islands in the HAZ began to decompose into ferrite and cementite as this region experienced a temperature of 411°C during FSW, and subsequently resulted in a structure consisting of tempered martensite in this region (figure 3(e)).

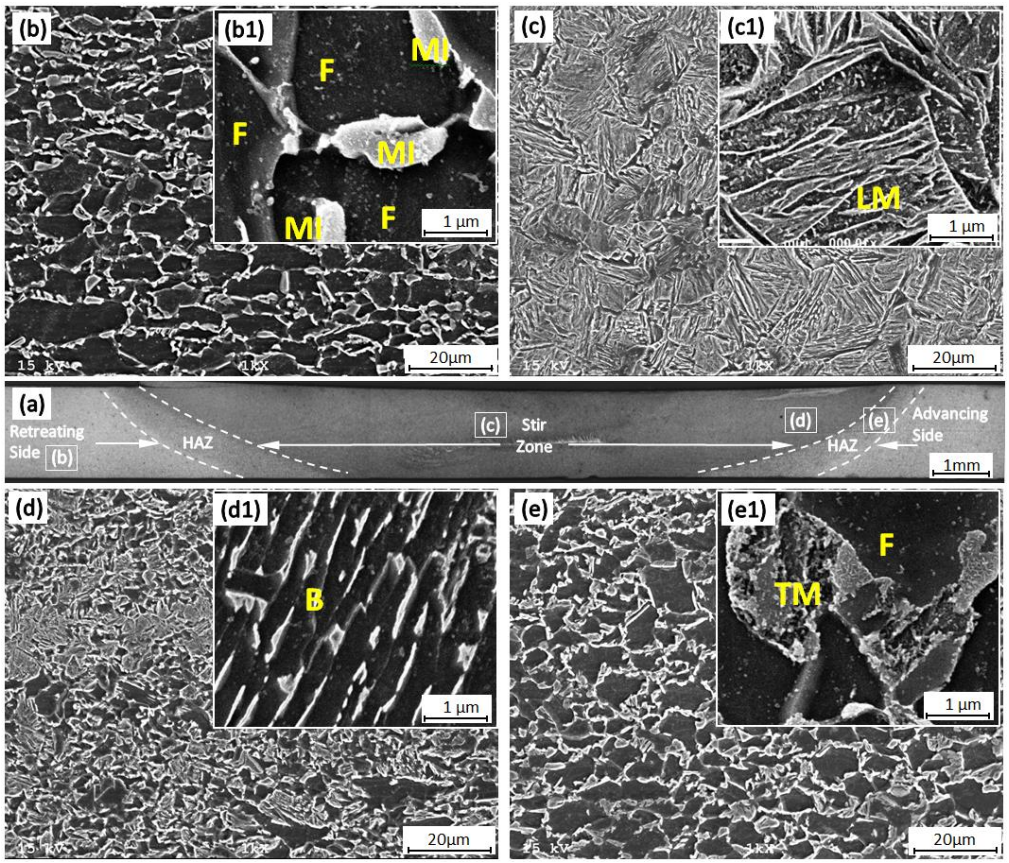

Figure 3. (a) Optical macrograph showing the cross-section of DP600 steel joint, (b)-(b1) SEM image of DP 600 steel base material microstructure, (c)-(c1) SEM image of the microstructure evolved in the SZ, (d)-(d1) SEM image of the microstructure of the SZ close to the HAZ, (e)-(e1) SEM image of the HAZ microstructure.

3.2. Microhardness and tensile properties

Optical macrograph of the weld region and a microhardness map with a color code illustrating the hardness distribution within the weld region are given in figures 4(a) and 4(b), respectively. A region corresponding to the geometry of the stirring tool in welded plate experienced significant plastic deformation and heat during FSW resulting in a drastic change in the microstructure as discussed above. This significant alteration in the microstructure in the stir zone led to a dramatic increase in the microhardness of this region. The hardness of the DP 600 steel base plate is about 220 HV. The region around the stirring tool tip subjected to severe plastic deformation, exhibiting a high hardness value (i.e. 400-450 HV), seen as yellow areas in figure 4(b). The presence of these local areas with a high hardness value within the weld region was also observed by other researchers [41,42] and they attributed this to the complex material flow and variation of plastic deformation from region to region, during FSW. The average hardness value of the stir zone was found to be about 400 HV. It was also observed that the microhardness in the stir zone decreased near the HAZ region. Thus, the average microhardness value in the SZ next to the HAZ was about 300 HV. The hardness of HAZ region, the microstructure of which composed of tempered martensite, displayed the lowest microhardness value, i.e., 205 HV. Although the hardness value of the HAZ was lower than that of the base plate, it was only 5% lower than that of the base material. Similar results were also reported by others [43,44]. Thus, it can be said that the hardness loss in the HAZ after FSW is less significant compared to the hardness loss experienced in fusion welding of this steel [43,44].

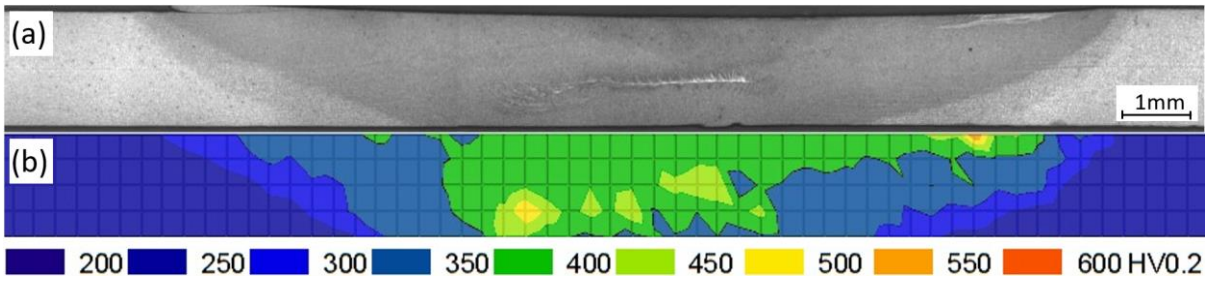

Figure 4. (a) A cross-section image of the FSWed sample, and (b) a contour map showing the microhardness distribution in the welded joint across the weld region.

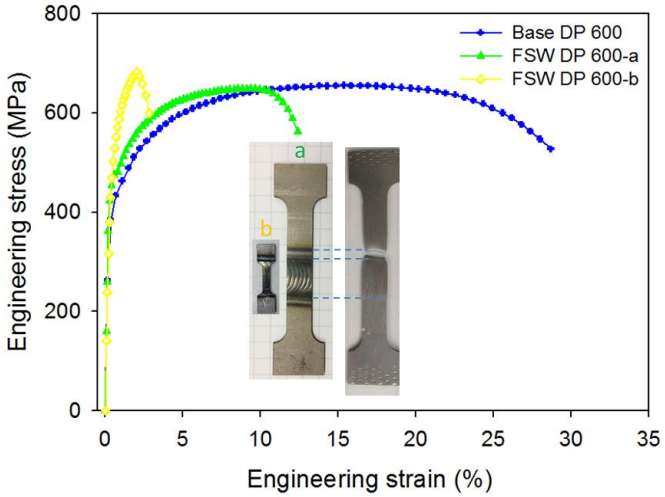

Figure 5. Engineering stress-strain curves obtained from base material specimen and friction stir welded samples (a: transverse tensile specimen and b: all-weld-metal tensile specimens).

The stress-strain curves of the base material and FSWed samples (both transverse tensile and all-weld-metal tensile specimens) are given in figure 5 and the strength and ductility values obtained from these curves are summarized in table 1. The base material exhibited a typical stress-strain curve of dual phase steel with high elongation and a large deformation hardening region. The yield strength and tensile strength values of the DP 600 steel base plate were 410 MPa and 645 MPa, respectively. Transverse tensile specimen (specimen a) failed in the transition region between the HAZ and base material, as seen in figure 5. The stress-strain curve displayed by the transverse tensile specimen is similar to that of the base material. This is not surprising since about two-thirds of the total gauge length of the transverse tensile specimen is the base material. The yield strength and tensile strength values obtained from the transverse tensile sample were 414 MPa and 640 MPa, respectively. These values are very similar to those of the base material since the failure took place away from the weld region between HAZ and BM due to strength overmatching nature of the joint as seen from the hardness distribution map of the joint (figure 4). This is not surprising since the joints with strength overmatching usually fail in the BM next to the weld region. Similar results were also reported for laser beam welded steel joints with strength overmatching [45-48] or for diffusion bonded joints with strength overmatching [49,50]. The elongation value exhibited by transverse tensile specimen extracted from the joint, however, showed a significantly lower total elongation to failure, i.e., 13%, than that of the base plate specimen, i.e., 28% (the reduction in elongation being 55%). This is due to the fact that the FSWed region (which is one-third of the total gauge length) having a yield stress of 590 MPa does not contribute to the total elongation during the

tensile test, this, in turn, leads to a reduction in the total elongation. Moreover, a 5% hardness drop in the HAZ compared to BM apparently led to early necking in the HAZ region next to the BM, and thus failure took place there. On the other hand, the stress-strain curve obtained from the all-weld-metal tensile specimen (sample b) exhibited a yield strength value of 590 MPa and a tensile strength of about 680 MPa. This result is in good agreement with the hardness distribution within the weld region. The reason for these relatively high strength values is apparently due to the evolution of hard microstructural constituents such as martensite and bainite within the weld region after FSW and to a lesser extent due to grain refinement.

Table 1. Tensile test results obtained.

Specimen	Yield Strength (MPa)	Tensile Strength (MPa)	Uniform Elongation (%)	Elongation to Failure (%)
DP 600 Base Plate	410 ± 6	645 ± 8	17 ± 1	28 ± 1
DP600-DP600-a (transverse tensile)	412± 7	640 ± 10	9 ± 2	13± 2
DP600-DP600-b (all-weld-metal)	590 ± 8	683 ± 12	3 ± 1	4 ± 1

4. Conclusions

DP 600 steel plates were joined by friction stir welding, and the microstructural evolutions, microhardness and tensile properties of the joint were investigated in detail. The main conclusions of this study can be summarized as follows:

- The DP 600 steel plates were successfully butt-joined by the FSW without any defects.
- The FSW led to a refined microstructure consisting of ferrite, bainite and lath martensite in the weld region due to dynamic recrystallization.
- Evolution of hard microstructural constituents in the weld region after FSW as well as grain refinement resulted in a significant increase in the hardness value within the weld region.
- The transverse tensile specimen failed within the transition region between the HAZ and the base material away from the stir zone (SZ). This is not a surprising due to the strength overmatching.
- All-weld-metal tensile specimen displayed very high yield and tensile strength values due to the evolution of hard phases within the weld region after FSW such as martensite and bainite. This is in good agreement with the hardness distribution across the weld region. On the other hand, this specimen exhibited a very low elongation.

Acknowledgments

This study was financed by the Scientific Research Projects Council of Karadeniz Technical University, under Grant No: FBA-2016-5509. Authors would like to thank Dr. Cemil Günhan ERHUY and Ermetal Automotive and Goods (ERMETAL) Inc., Bursa, Turkey for their support in supplying the initial material.

References

[1] Rashid M S 1981 Dual phase steels *Ann. Rev. Mater. Sci.* **11** 245-67
[2] Kim N J and Thomas G 1981 Effects of morphology on the mechanical behavior of a dual phase Fe/2Si/0.1 C steel. *Metall. Trans. A* **12** 483-9
[3] Coldren A P and Tither G 1978 Development of a Mn-Si-Cr-Mo as-rolled dual-phase steel *J. Met.* **30** 6-9
[4] Nishimoto A, Hosoya Y and Nakaoka K 1981 A new type of dual-phase steel sheet for automobile outer body panels *Trans. Iron Steel Inst. Japan* **21** 778-82
[5] Antunes W D, Sergio M and Lima F De 2016 Experimental development of dual phase steel laser-

arc hybrid welding and its comparison to laser and gas *Metal Arc Welding* **21** 379-86
[6] Ghosh M, Gupta R K and Husain M M 2014 Friction stir welding of stainless steel to al alloy: Effect of thermal condition on weld nugget microstructure *Metall. Mater. Trans. A Phys. Metall. Mater. Sci.* **45** 854-63
[7] Kashaev N, Ventzke V and Çam G 2018 Prospects of laser beam welding and friction stir welding processes for aluminum airframe structural applications *J. Manuf. Process.* **36** 571-600
[8] Çam G and Ipekoglu G 2017 Recent developments in joining of aluminum alloys *Int. J. Adv. Manuf. Technol.* **91** 1851-66
[9] Cam G and Mistikoglu S 2014 Recent developments in friction stir welding of al-Alloys *J. Mater. Eng. Perform.* **23** 1936-53
[10] Cam G 2011 Friction stir welded structural materials: Beyond Al-alloys *Int. Mater. Rev.* **56** 1-48
[11] Çam G, Ipekoglu G, Küçükömeroglu T and Aktarer S M 2017 Applicability of friction stir welding to steels *J. Achiev. Mater. Manuf. Eng.* **80** 65-85
[12] Çam G 2005 Friction stir welding: A novel welding technique developed for Al-alloys *Mühendis ve Makine (Engineer Mach.)* **46** 30-9
[13] Günen A, Kanca E, Demir M, Demir M, Çavdar F, Mistikoğlu S and Çam G 2018 Microstructural and mechanical properties of friction stir welded pure lead *Indian J. Eng. Mater. Sci.* **25** 26-32
[14] Küçükömeroglu T, Sentürk E, Kara L, Ipekoglu G and Çam G 2016 Microstructural and mechanical properties of friction stir welded nickel-aluminum bronze (NAB) alloy *J. Mater. Eng. Perform.* **25** 320-6
[15] Çam G, Mistikoglu S and Pakdil M 2009 Microstructural and mechanical characterization of friction stir butt joint welded 63% Cu-37% Zn Brass Plate *Weld. J.* **88** 225-32
[16] Çam G, Serindag H T, Mistikoglu S and Yavuz H 2008 The effect of weld parameters on friction stir welding of brass plates *Mat.-wiss. u. Werkstofftech* **39** 394-9
[17] Xie G M, Ma Z Y and Geng L 2008 Effect of microstructural evolution on mechanical properties of friction stir welded ZK60 alloy *Mater. Sci. Eng. A* **486** 49-55
[18] Bozkurt Y, Salman S and Çam G 2013 Effect of welding parameters on lap shear tensile properties of dissimilar friction stir spot welded AA 5754-H22/2024-T3 joints *Sci. Technol. Weld. Join.* **18** 337-45
[19] Çam G, İpekoğlu G and Serindağ H T 2014 Effects of use of higher strength interlayer and external cooling on properties of friction stir welded AA6061-T6 joints *Sci. Technol. Weld. Join.* **19** 715-20
[20] Çam G, Güçlüer S, Çakan A and Serindag H T 2009 Mechanical properties of friction stir butt-welded Al-5086 H32 plate *Mat.-wiss. U. Werkstofftech* **40** 638-42
[21] İpekoğlu G, Erim S and Çam G 2014 Effects of temper condition and post weld heat treatment on the microstructure and mechanical properties of friction stir butt-welded AA7075 Al alloy plates *Int. J. Adv. Manuf. Technol.* **70** 201-13
[22] İpekoğlu G, Erim S and Çam G 2014 Investigation into the influence of post-weld heat treatment on the friction stir welded AA6061 Al-alloy plates with different temper conditions *Metall. Mater. Trans. A* **45** 864-77
[23] İpekoğlu G, Gören Kıral B, Erim S and Çam G 2012 Investigation of the effect of temper condition on friction stir weldability of AA7075 Al-alloy plates *Mater. Teh.* **46** 627-32
[24] İpekoğlu G, Erim S, Gören Kıral B and Çam G 2013 Investigation into the effect of temper condition on friction stir weldability of AA6061 Al-alloy plates *Kov. Mater* **51** 155-63
[25] Küçükömeroğlu T, Aktarer S M, İpekoğlu G and Cam G 2018 Mechanical properties of friction stir welded St 37 and St 44 steel joints *Mater. Test.* **60** 1163-70
[26] Mishra R S and Ma Z Y 2005 Friction stir welding and processing *Mater. Sci. Eng. R Reports* **50** 1-78
[27] Küçükömeroğlu T, Aktarer S M, İpekoğlu G and Çam G 2018 Microstructure and mechanical properties of friction-stir welded St52 steel joints *Int. J. Miner. Metall. Mater.* **25** 1457-64

[28] Nene S S, Liu K, Frank M, Mishra R S, Brennan R E, Cho K C, Li Z and Raabe D 2017 Enhanced strength and ductility in a friction stir processing engineered dual phase high entropy alloy *Sci. Rep.* **7** 16167
[29] Tehrani-Moghadam H G, Jafarian H R, Salehi M T and Eivani A R 2018 Evolution of microstructure and mechanical properties of Fe-24Ni-0.3C TRIP steel during friction stir processing *Mater. Sci. Eng. A* **718** 335-44
[30] Razmpoosh M H, Zarei-Hanzaki A and Imandoust A 2015 Effect of the Zener–Hollomon parameter on the microstructure evolution of dual phase TWIP steel subjected to friction stir processing *Mater. Sci. Eng. A* **638** 15-9
[31] Xie G M, Cui H B, Luo Z A, Yu W, Ma J and Wang G D 2016 Effect of Rotation Rate on Microstructure and Mechanical Properties of Friction Stir Spot Welded DP780 Steel *J Mater Sci Technol.* **32** 326–32
[32] Feng Z, Santella M L, David S A, Steel R J, Packer S M, Pan T-Y, Kuo M and Bhatnagar R S 2005 Friction stir spot welding of advanced high-strength steels - A feasibility study *SAE Tech. Pap.* **1** 1-7
[33] Saunders N, Miles M, Hartman T, Hovanski Y, Hong S-T and Steel R 2014 Joint strength in high speed friction stir spot welded DP 980 steel *Int. J. Precis. Eng. Manuf.* **15** 841-8
[34] Santella M, Hovanski Y, Frederick A, Grant G and Dahl M 2010 Friction stir spot welding of DP780 carbon steel **15** 271-8
[35] Khan M I, Kuntz M L, Su P, Gerlich A, North T and Zhou Y 2007 Resistance and friction stir spot welding of DP600: A comparative study *Sci. Technol. Weld. Join.* **12** 175-82
[36] Das H, Mondal M, Hong S-T, Lim Y and Lee K-J 2018 Comparison of microstructural and mechanical properties of friction stir spot welded ultra-high strength dual phase and complex phase steels *Mater. Charact.* **139** 428-36
[37] Miles M P, Pew J, Nelson T W and Li M 2006 Comparison of formability of friction stir welded and laser welded dual phase 590 steel sheets *Sci. Technol. Weld. Join.* **11** 384-8
[38] Kucukomeroglu T and Aktarer S M 2017 Microstructure, microhardness and tensile properties of FSWed DP 800 steel *J. Achiev. Mater. Manuf. Eng.* **81** 56-60
[39] Ohashi R, Fujimoto M, Mironov S, Sato Y S and Kokawa H 2009 Effect of contamination on microstructure in friction stir spot welded DP590 steel *Sci. Technol. Weld. Join.* **14** 221-7
[40] Xie G M, Cui H B, Luo Z A, Yu W, Ma J and Wang G D 2015 Effect of rotation rate on microstructure and mechanical properties of friction stir spot welded DP780 steel *J. Mater. Sci. Technol.* **32** 326-32
[41] Cho J-H, Boyce D E and Dawson P R 2005 Modeling strain hardening and texture evolution in friction stir welding of stainless steel *Mater. Sci. Eng. A* **398** 146-63
[42] Tutunchilar S, Haghpanahi M, Givi M K B, Asadi P and Bahemmat P 2012 Simulation of material flow in friction stir processing of a cast Al–Si alloy *Mater. Des.* **40** 415-26
[43] Pazooki A M A, Hermans M J M, Richardson I M, Pazooki A M A, Hermans M J M and Richardson I M 2016 Finite element simulation and experimental investigation of thermal tensioning during welding of DP600 steel Finite element simulation and experimental investigation of thermal tensioning during welding of DP600 steel *Sci. Technol. Weld. Join.* **22** 7-21
[44] Xu W, Westerbaan D, Nayak S S, Chen D L, Goodwin F and Zhou Y 2013 Tensile and fatigue properties of fiber laser welded high strength low alloy and DP980 dual-phase steel joints *Mater. Des.* **43** 373-83
[45] dos Santos J, Çam G, Torster F, Insfran A, Riekehr S, Ventzke V and Koçak M 2000 Properties of power beam welded steels, al-and ti-alloys: Significance of strength mismatch *Weld. World* **44** 42-64
[46] Çam G, Erim S, Yeni Ç and Koçak M 1999 Determination of mechanical and fracture properties of laser beam welded steel joints *Weld. J.* **79** 193-201
[47] Çam G, Yeni Ç, Erim S, Ventzke V and Koçak M 1998 Investigation into properties of laser

welded similar and dissimilar steel joints *Sci. Technol. Weld. Join.* **3** 177-89
[48] Çam G, Koçak M and dos Santos J 1999 Developments in laser welding of metallic materials and characterization of the joints *Weld. World* **43** 13-26
[49] Çam G, Koçak M, Dobi D, Heikinheimo L and Sirén M 1997 Fracture behaviour of diffusion bonded bimaterial Ti–Al joints *Sci. Technol. Weld. Join.* **2** 95-101
[50] Koçak M, Pakdil M and Çam G 2002 Fracture behaviour of diffusion bonded titanium alloys with strength mismatch *Sci. Technol. Weld. Join.* **7** 187-96